Redesign and improved performance of the tropospheric ozone lidar at the Jet Propulsion Laboratory Table Mountain Facility

I. Stuart McDermid, Georg Beyerle, David A. Haner, and Thierry Leblanc

Improvements to the tropospheric ozone lidar at the Jet Propulsion Laboratory Table Mountain Facility for measurements of ozone profiles in the troposphere and lower stratosphere, between approximately 5- and 20-km altitude, are described. The changes were primarily related to the receiver optical subsystems and the data-acquisition system. The original 40-cm Cassegrain telescope was replaced with a faster ($f/3$) 91-cm Newtonian mirror. In the focal plane of this mirror, the lidar signal is divided into two parts by use of two separate optical fibers as field stops corresponding to different but neighboring 0.6-mrad fields of view. We then separate the two received wavelengths by aligning each transmitted beam to one of the fibers. In addition, two 50-mm telescopes are used for the collection of near-range returns. The four optical signals are brought to a chopper wheel for independent signal selection in the time and range domain. For each channel, an interference filter is used for skylight rejection and additional cross-talk prevention. The signals are detected with miniature photomultiplier tubes and input to a fast photon-counting system. The goals of these modifications were to increase the spatial and temporal resolution of the lidar, to extend the altitude range covered, to improve the quality of the raw data, and to enable regular and routine operation of the system for long-term measurements. © 2002 Optical Society of America

OCIS codes: 010.0010, 010.4950, 010.7030, 010.3640, 280.1910.

1. Introduction

Several lidar systems are operated at the Jet Propulsion Laboratory (JPL) Table Mountain Facility (TMF; 34.4 °N, 117.4 °W) for atmospheric measurements in the troposphere and stratosphere.[1,2] One of these is a differential absorption lidar (DIAL) system for ozone profiling and another is an elastic and Raman scattering system primarily for aerosol and cloud observations.[3,4] Previously these two lidars were combined in a single system, which involved many problems and compromises and limited their performance. Recently these systems were redesigned and separated to improve their capabilities.

In particular, the entire optical receivers, including the telescopes and data-acquisition systems, were replaced to take advantage of newer technologies. The goals of these modifications were to increase the spatial and temporal resolution of the lidars, to extend the altitude range covered, and to improve the quality of the raw data. In this paper we discuss the improvements to the tropospheric ozone DIAL.

The ozone DIAL system uses a dual-beam Raman-shifted Nd:YAG[2] for the transmitter with a four-channel receiver. The original system used a single 40-cm aperture Cassegrain telescope operating in an afocal (beam compressor) mode with the collimated output directed onto a concave holographic grating.[1] In this configuration the zero-order reflection from the grating provided the aerosol channels, and the first-order refracted light was used for the ozone DIAL channels. In an intermediate step, a second 45-cm aperture Newtonian telescope was added, and the aerosol channels were moved to this receiver. Subsequently, the ozone DIAL system was operated in an alternating pulse, λ_1/λ_2, mode so that a single detector could be used in place of the spectrometer.[5] Although this arrangement had some advantages, it significantly increased the required integration

When this research was performed, the authors were with the Table Mountain Facility, Jet Propulsion Laboratory, California Institute of Technology, P.O. Box 367, Wrightwood, California 92397. G. Beyerle is now with the Division Kinematics and Dynamics of the Earth, GeoForschungsZentrum, Telegrafenberg A17/PB1.1, D-14473 Potsdam, Germany. The e-mail address for I. S. McDermid is mcdermid@tmf.jpl.nasa.gov.

Table 1.   Primary Mirror Specifications

Diameter	0.91 m (36 in.)
Focal length	2.54 m (100 in.)
Surface	Parabolic
Edge thickness	41 mm (1.625 in.)
Center thickness	20 mm (0.813 in.)
Substrate	Pyrex
Thermal expansion coefficient	$3.3 \ 10^{-6} \ K^{-1}$
Coating	AlSiO
Image spot size	<1 mm (90% of light intensity)

times.   Here we describe yet another configuration for this ozone DIAL system but one that provides the performance and high-quality data we have been seeking.   Having operated continuously now since November 1999, it is expected that this new configuration will remain stable for the foreseeable future.

2.   Lidar Modifications

A.   Laser Transmitter

The laser transmitter for the ozone DIAL system is essentially unchanged from that described by McDermid et al.[1]   The DIAL wavelengths are generated by stimulated Raman shifting of the Nd:YAG fourth harmonic (266 nm) in D_2 (289 nm), HD (294 nm), or H_2 (299 nm).[2]   The laser is a 10-Hz dual-beam system, and the two output wavelengths are generated and transmitted simultaneously.   Originally this laser produced 100 mJ of energy at 266 nm in each beam.   However, the performance has degraded over the years, and the results described in this paper were obtained with less than half of this energy.   To reduce the laser divergence, as is required because of the small field of view (FOV) of the telescope, refractive beam expander telescopes with a magnification of 5 are used after the Raman cells.

B.   Telescope

The telescope was replaced to both increase the aperture and improve the quality of the image.   From considerations of simplicity and cost it was decided to use a Newtonian configuration.   The mirror was made by Intermountain Optics (Murray, Utah) and is 91 cm (36 in.) in diameter with a focal length of 254 cm (100 in.), i.e., $f/3$.   Thus the light gathering capacity was immediately increased by more than a factor of 5 compared with the 40-cm telescope.   Specifications of the mirror are given in Table 1.   Because the telescope is required to look vertically upwards only, the mirror is supported on its back surface by a stiff, flat optical breadboard.   A thin layer of air bubbles between the rear surface of the mirror and the breadboard accommodates any small inconsistencies in the flatness of the back surface.

The telescope structures were designed and built at TMF following some of the guidelines developed by Steinbach et al.[6] for large lidar telescopes.   The focal-plane optics are supported by a hexapod structure as shown in Fig. 1.   An analysis and optimization of the hexapod design was carried out with
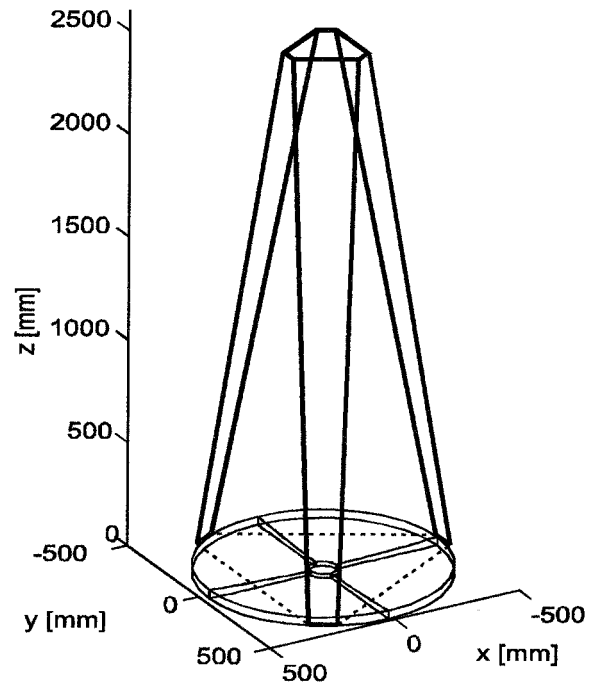
Fig. 1.   Design and dimensions of the telescope hexapod structure.

MATLAB programs from the Sandia Hexapod Project.[7] The hexapod rods were made from stainless steel to reduce thermal-expansion effects.   This structure is extremely rigid even with relatively small-diameter (25-mm) rods.

C.   Fiber Coupling

A custom dual-fiber arrangement (CeramOptec) is mounted at the telescope focus as shown schematically in Fig. 2.   In this arrangement the fiber jacket is stripped away at the ends so that the fibers can essentially touch.   The fibers are then held in place in a special stainless-steel ferrule (6 mm diameter × 50 mm long).   The fiber core diameters are 1.5 mm and are used as the effective field stops at the telescope focus.   Figure 3 shows the resulting FOV projected into the atmosphere.   Each fiber views a different region in the atmosphere, but, because the FOV is only 600 μrad, these regions are small and close together, e.g., at 10 km each region is 6 m in diameter and separated by essentially the same amount.   This arrangement is then used as the pri-
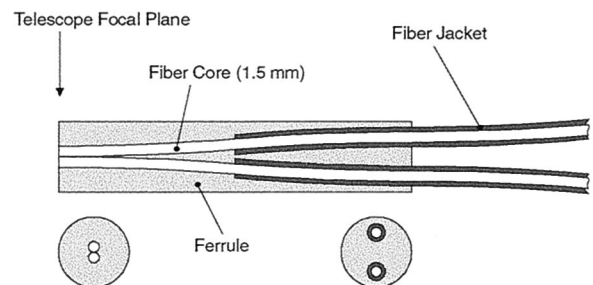
Fig. 2.   Dual-fiber arrangement, located at the telescope focus.
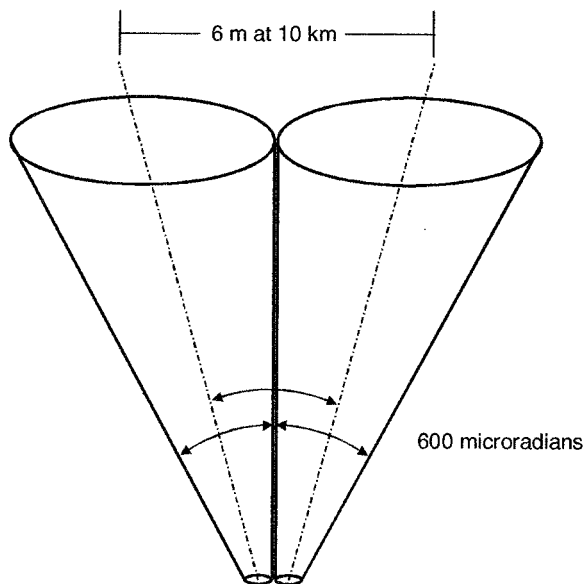
Fig. 3. Schematic diagram of the FOV of the twin fibers, projected into the atmosphere.

mary step to separate the two DIAL wavelengths. The transmitted beams are each aligned to one particular fiber, i.e., centered in the FOV (see Figs. 3 and 4). Because the laser divergence is much less than the FOV, the beams are well separated in the atmosphere. One advantage of this method of separating the different wavelengths spatially is that it is wavelength independent. However, it does make some assumptions with regard to the DIAL method. These are that the atmosphere is homogeneous through the different volumes probed by each beam or that movement of the atmosphere during the integration time will act to average out any differences (compare with pulsing alternate wavelengths). We believe the combination of these assumptions to be highly defensible, especially considering how close together they actually are and the fact that typical integration times are >1 h. Figure 4 shows the geometric spot patterns from a ray trace program of the image of the laser beams at different altitudes on the twin fibers at the telescope focus. Even though the separation between the axes of the transmit optics and the large telescope is quite small, ~0.6 m, this is still a biaxial system and thus
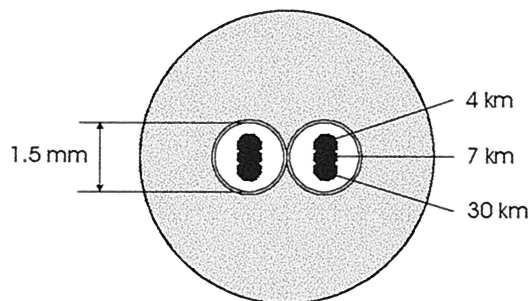
Fig. 4. Geometric ray trace spot diagrams of the image from different altitudes on the dual fibers at the telescope focus.
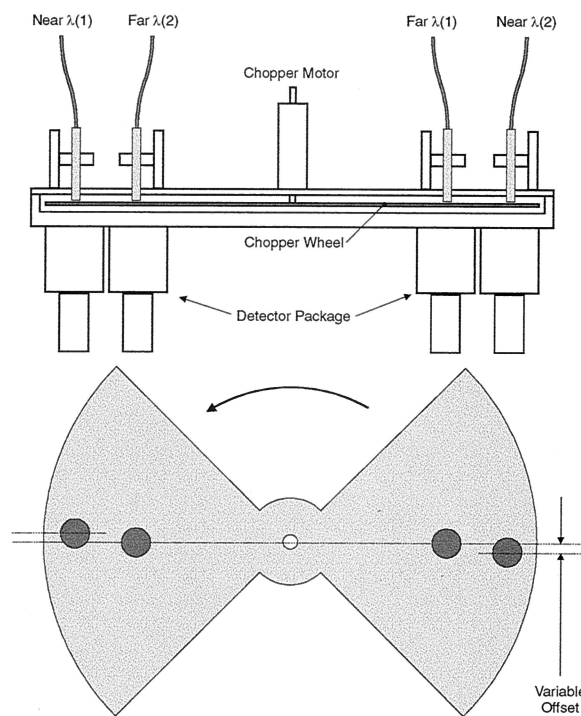
Fig. 5. Arrangement of the fibers, chopper wheel, and detector packages.

the image from different altitudes moves across the focal plane. However, Fig. 4 shows that the 1.5-mm diameters of the fibers are more than adequate to encompass returns from all altitudes of interest.

Returns from close range are collected by two separate small telescopes, of 50-mm aperture, that focus the laser backscatter onto 400 μm-diameter fibers. Each of these small telescopes is aligned independently to one of the output laser beams. Thus the lidar signal is divided into four fibers: near range $\lambda(1)$ and $\lambda(2)$ and far range $\lambda(1)$ and $\lambda(2)$. The fibers are then brought to a rotating chopper as shown in Fig. 5.

D. Chopper

The chopper wheel rotates at 6000 rpm, and the radii to the fiber positions are 160 mm for the near-range fibers and 100 mm for the far-range fibers. The near- and far-range chopping positions are staggered such that the far range opens up at an approximately 5-km-higher altitude. Adjustment is provided so that this offset can be both varied and set precisely. At the near-range fiber positions the blade speed is ~ 100 m s^{-1}, and therefore the time to move across the 400-μm fiber is 4 μs, i.e., <1 km. This fast transition is required so that we can get the near channels open as soon as possible while still blocking the returns from the boundary layer and scattered laser light within the laboratory (see Section 3).

E. Detectors

A detector package is attached to the rear of the chopper housing. This package, shown in Fig. 6,
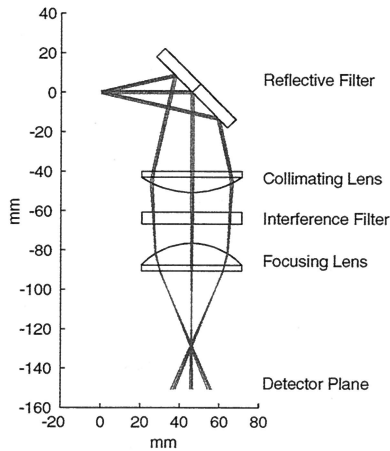
Fig. 6. Details of the detector optics. The photomultiplier is located at the detector plane.

incorporates a narrowband mirror that reflects the UV light at the laser wavelengths and transmits everything else; this helps to reduce background noise from skylight. This is followed by a collimating lens and a narrowband interference filter. The light is then refocused onto the photocathode (8 mm ϕ) of a photomultiplier module (Hamamatsu H5783P-06). Signals from the photomultipliers are input directly to a four-channel photon-counting system (Licel). The minimum dwell time of the Licel multichannel scaler is 50 ns, corresponding to a range resolution of ~7.5 m; however, typically eight or ten channels are binned together internally for a maximum resolution of 60 or 75 m.

3. Results

An example of nighttime raw data obtained by this lidar system for a 2-h integration, 02:52–04:52 (UT) on 19 March 2000, is shown in Fig. 7. Of particular note is the dynamic range of the lidar signals, which extends over six decades, primarily because of the low background signal. These profiles are typical of those obtained by this lidar for nighttime measure-
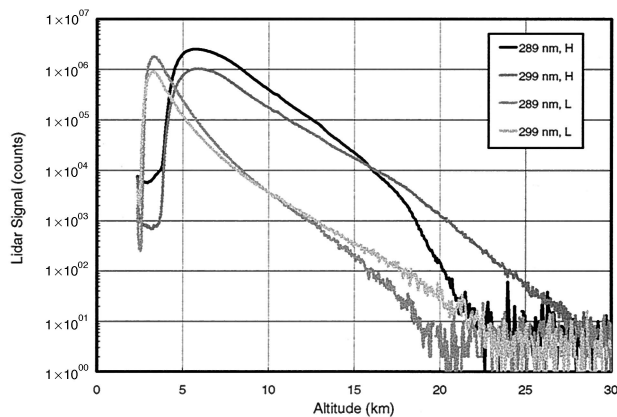
Fig. 7. Typical nighttime raw data curves from a 2-h integration (19 March 2000, 02:52–04:52 UT). Note that the altitude of the TMF is 2.3 km.

ments. The upper altitude limit is set by the extinction of the laser radiation by the increasing concentration of ozone above 20 km; the 289-nm beam is completely extinguished by the ozone layer as can clearly be seen in the raw data plots. To reach higher altitudes a second DIAL system with use of longer wavelengths, 308 and 355 nm, is used. The integration time for these profiles was ~2 h; however, much shorter times can be used to reach lower altitudes.

Figure 7 also demonstrates the operation of the optical chopper. The single chopper wheel independently shuttered each of the four data curves shown. There is no electronic gating in this system, and the turn-on transitions are solely due to the mechanical chopper. The low channels signals are usable from ~4 km upwards and the high channels from ~8 or 9 km upwards.

Typical tropospheric ozone profiles are shown in Fig. 8. The upper panel shows two profiles, derived from the lower-intensity (small telescopes, red curve) signals and the higher-intensity (large telescope, blue curve) signals. The low profile extends from ~5 to 17 km and the high profile from ~9 to 20 km. This example, from 3 January 2001, was chosen because there are significant features in the ozone profile that can be used to demonstrate the agreement between the separate profiles in the regions where they overlap.

A second DIAL system, operating at 308 and 355 nm, for ozone measurements in the stratosphere, ~15 − >50 km altitude, has also been in long-term operation at JPL TMF.[1,8–13] It has proved possible to operate both the tropospheric and the stratospheric ozone lidars simultaneously, without interference between the systems. This provides a novel opportunity to combine the signals from the two separate lidars to create new DIAL wavelength pairs. The combination of the 299-nm signal from the troposphere system with the 355-nm signal from the stratosphere lidar provides a high-quality profile over the altitude region from ~15 to 30 km, which is also shown in Fig. 8 (green curve). This hybrid profile is useful when the profiles from the two systems are combined to give a single profile all the way from ~5-km to >50-km altitude, as shown in Fig. 9 with data from 2 October 2001, 03:11–05:11 (UT). In Fig. 9, the red and blue curves are the profiles from the tropospheric lidar (289–299 nm), the magenta and cyan curves are from the stratospheric system (308–355 nm), and the green curve is the hybrid profile (299–355 nm) described above. It can be seen that there is excellent agreement between the profiles in the regions where they overlap, allowing them to be combined to give the single atmospheric ozone profile shown in the lower panel of Fig. 9.

4. Conclusion

The modified tropospheric lidar has been making routine measurements since November 1999,[8,14] and the results are being archived at the Network for the Detection of Stratospheric Change data center. The re-
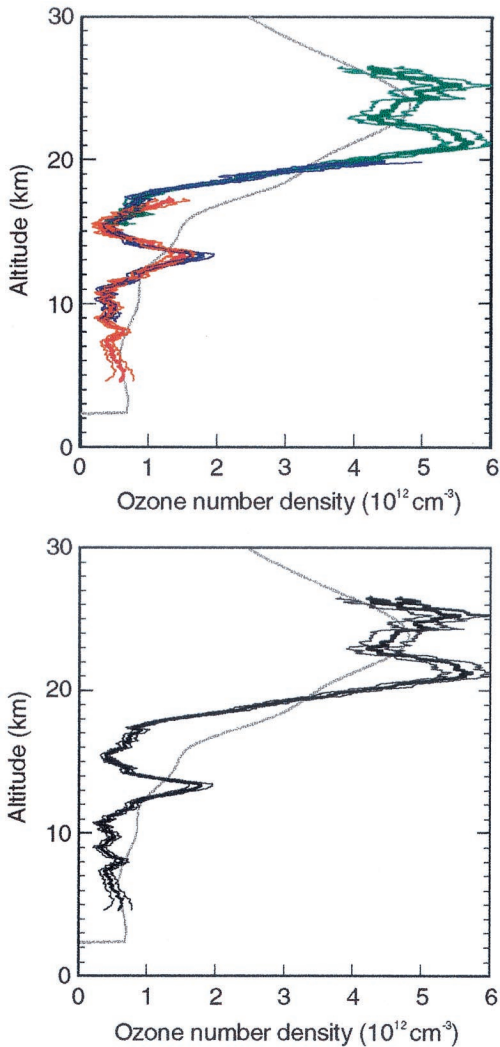
Fig. 8. Upper panel: ozone profiles (3 January 2001, 03:46–05:19 UT) from (red) the 289–299-nm pair, small telescopes; (blue) same but for the large telescope; (green) hybrid 299–355-nm pair. Note agreement in regions of overlap. Lower panel: composite troposphere and lower-stratosphere ozone profile.

Fig. 9. Complete atmospheric ozone profile, 5–55 km (2 October 2001, 03:11–05:11 UT). Upper panel shows the five profile segments: two tropospheric (red, blue; 289–299 nm), two stratospheric (cyan, magenta; 308–355 nm), and one hybrid (green; 299–355 nm) that are combined to give the composite profile shown in the lower panel. Inset shows upper section on a logarithmic scale.

design of the lidar receiver has resulted in significantly higher signal-to-noise ratios compared with the previous design, allowing profiles to be measured up to 20-km altitude with the tropospheric system alone. Through simultaneous operation of the tropospheric and stratospheric DIAL systems, an ozone profile from 4 km to >50 km can be obtained from a 2-h nighttime integration. The ongoing plan is to make regular measurements on two to three nights per week. Special campaigns will be launched as required, for example, for validation programs. We also plan campaigns to detect and observe polar vortex filaments passing over Table Mountain[15]; historical results indicate that this is not an unusual occurrence in the springtime when the Arctic vortex breaks down.

References

1. I. S. McDermid, D. A. Haner, M. M. Kleiman, T. D. Walsh, and M. L. White, "Differential absorption lidar systems at JPL-TMF for tropospheric and stratospheric ozone measurements," Opt. Eng. **30,** 22–30 (1991).

2. D. A. Haner and I. S. McDermid, "Stimulated Raman shifting of Nd:YAG fourth harmonic (266 nm) in H_2, HD and D_2," IEEE J. Quantum Electron. **26,** 1292–1298 (1990).

3. G. Beyerle, I. S. McDermid, R. Neuber, and P. von der Gathen, "Comparative study of stratospheric aerosols and ozone at mid

and high latitudes during the Pinatubo episode, 1991–1994," in *Advances in Atmospheric Remote Sensing with Lidar*, A. Ansmann, R. Neuber, P. Rairoux, and U. Wandinger, eds. (Springer, New York, 1996), pp. 489–492.

4. G. Beyerle, M. R. Gross, D. A. Haner, N. T. Kjome, I. S. Mc-Dermid, T. J. McGee, J. M. Rosen, H.-J. Schäfer, and O. Schrems, "A lidar and backscatter sonde measurement campaign at Table Mountain during February-March 1997: observations of cirrus clouds," Bull. Am. Meteorol. Soc. **58,** 1275–1287 (1998).

5. M. H. Proffitt and A. O. Langford, "Ground-based differential absorption lidar system for day or night measurements of ozone throughout the free troposphere," Appl. Opt. **36,** 2568–2585 (1997).

6. M. Steinbach, U. Bräuer, H. Fischer, C. Hüllenkremer, H.-D. Kleinschrodt, W. Mildner, R. Ponzer, H.-J. Schäfer, G. Sesselmann, and F. Theopold, "Special features of large lidar telescopes," in *Lidar and Atmospheric Sensing*, R. J. Becherer, ed., Proc. SPIE **2505,** 66–74 (1995).

7. Sandia Hexapod Project, http://ppsc.pme.nthu.edu.tw/~tclee/mirror/Sandia/hexapod.html.

8. I. S. McDermid and T. Leblanc, "An overview of 10 years of lidar measurements at Table Mountain Facility, California, and Mauna Loa Observatory, Hawaii," presented at the Network for the Detection of Stratospheric Change Symposium 2001, Arcachon, France, 24–27 September 2001.

9. I. S. McDermid, S. M. Godin, and L. O. Lindquist, "Ground-based laser DIAL system for long-term measurements of stratospheric ozone," Appl. Opt. **29,** 3603–3612 (1990).

10. I. S. McDermid, "Ground-based lidar and atmospheric studies," Geophys. Surv. **9,** 107–122 (1987).

11. I. S. McDermid, S. M. Godin, and T. D. Walsh, "Lidar measurements of stratospheric ozone and intercomparisons and validation," Appl. Opt. **29,** 4914–4923 (1990).

12. I. S. McDermid, "NDSC and the JPL stratospheric lidars," Rev. Laser Eng. **23,** 97–103 (1995).

13. T. Leblanc and I. S. McDermid, "Stratospheric ozone climatology from lidar measurements at Table Mountain (34.4 °N, 117.7 °W) and Mauna Loa (19.5 °N, 155.6 °W)," J. Geophys. Res. **105,** 14613–14623 (2000).

14. I. S. McDermid, G. Beyerle, D. A. Haner, and T. Leblanc, "Redesign and improved performance of the tropospheric ozone lidar at Table Mountain," presented at the Quadrennial Ozone Symposium, Sapporo, Japan, 3–8 July 2000.

15. A. Hauchecorne, S. Godin, M. Marchand, B. Heese, and C. Souprayen, "Quantification of the transport of chemical constituents from the polar vortex to middle latitudes in the lower stratosphere using the high-resolution advection model MIMOSA and effective diffusivity," J. Geophys. Res. (to be published).